SEGi Review ISSN 1985-5672
Vol. 5, No. 1, July 2012, 29-40
*Corresponding author. E-mail: jjfoo@segi.edu.my

FORCED CONVECTIVE HEAT TRANSFER ENHANCEMENT WITH PERFORATED PIN FINS SUBJECT TO AN IMPINGING FLOW

***Ji-Jinn Foo[1, 2], Shung-Yuh Pui[1], Yin-Ling Lai[1], Swee-Boon Chin[2]**
[1]School of Engineering, SEGi University College, Selangor, Malaysia;
[2]Department of Mechanical Engineering, Sheffield University, Sheffield, United Kingdom.

ABSTRACT

The rapid growth in high speed multi-functional miniaturized electronics demands more stringent thermal management. The present work numerically investigates the use of staggered perforated pin fins to enhance the rate of heat transfer while subject to a vertical impinging flow. In particular, the number of horizontal perforations and the vertical and horizontal diameters of perforation on each pin are studied. Results show that the Nusselt number of pins with horizontal and vertical perforations is about 9% higher than that for the solid pins and it increases with the number of horizontal perforations. Pressure drop with perforated pins is reduced by about 10% compared with that in solid pins. Perforation produces smaller but larger number of vortices downstream of the pins which increases convective heat transfer but reduces pressure losses. However, further increasing the perforation diameters leads to a significant drop in thermal dissipation. Overall, pin fins with vertical and horizontal perforations are preferred for heat sink facing an oncoming vertical flow.

1.0 Introduction

Heat sinks are employed to dissipate thermal energy generated by electronic components to maintain a stable operation temperature. A compact, efficient and easily fabricated heat sink is required. However, the design of heat sink device is strongly dependent upon the need to balance thermal dissipation and pressure drop across the system such that the overall cost and efficiency may be optimized. An example of a familiar solution is to apply pin fin array onto a heat sink design.

Kim *et. al*. [1] studied experimentally the thermal dissipation performance of plate fin and pin fin heat sinks when subject to a vertical impinging flow. Their results showed that at small pumping power, the heat sink thermal resistance is lower for pin fins compared with that for the plate fins. The inlet geometry of confined impinging flow on a smooth channel is found to be sensitive to heat transfer, where the inlet channel width and nozzle-to-plate spacing decrease with increasing Nusselt number and pressure drop [2]. Yang and Peng [3] investigated numerically the impinging heat transfer performance of heat sink with un-uniform fin width. They found that the effect of fin dimensions on forced convective heat transfer is more obvious at high Reynolds number.

Sparrow *et. al*. [4] obtained experimentally the effects of in-line and staggered pin fin arrays on thermal dissipation and pressure drop. They concluded that the heat transfer and pressure coefficients for staggered arrays are higher than those for the in-line arrangement. Tahat *et. al*. [5] optimized the lengthwise and spanwise arrangements of staggered and in-line pins. Soodphakdee *et. al*. [6] reported numerically that at low Reynolds number

(Re_{Dh}<390), higher heat transfer coefficient is obtained with elliptical pin fins. However, at high Re_{Dh} circular pin fins is more effective. Yang *et. al*. [7] studied numerically forced convective heat transfer in staggered aluminum porous pin fin arrays. They found higher heat transfer rate in porous pin fins than in solid pins. Wake formation behind pin is minimal leeward of porous pin consequently minimizing pressure losses across the heat sink. Their results supported the earlier experimental study carried out by Sahin and Demir [8]. The pressure coefficient for staggered pin fin array can be reduced by either introducing perforated pin-fins or pin-fin-dimple arrays [9, 10]. Recently, Yong *et. al*. [10] found from experimental and numerical studies that in horizontally perforated pin fin arrays subject to parallel incoming flow, increasing the number of perforation is more important than increasing perforation diameter.

The present paper focuses on numerical study of forced convective heat transfer in staggered perforated pin fins array subject to a vertical impinging flow. The effects of number of horizontal perforation and the horizontal and vertical perforation diameters on the rate of thermal dissipation and pressure drop are investigated and compared with those for the solid pins.

2.0 Numerical Method

A proprietary software package ANSYS-FLUENT (version 12.1.4, USA) was employed to investigate the three-dimensional (3D), laminar, steady-state and incompressible forced convective heat transfer of staggered and perforated pin fins. The schematic diagram of the symmetric computational domain is shown in Fig. 1. The vertical inlet internal channel dimensions are $100 \times 100 \times 70$mm in length, width and height, respectively. The horizontal internal channel is $1300 \times 106 \times 67$mm. The surrounding walls are of 3mm thick. Heat transfer performance was simulated on four sets of staggered pin fin arrays, viz (i) solid pins, Fig. 2(a), (ii) pins with 1 to 5 horizontal perforation each of 4mm diameter, Fig. 2(b), (iii) pins of 2, 3, 4 and 5mm horizontal perforation diameter with 5 perforations on each pin, Fig. 2(c), and (iv) pins of 2, 3, 4 and 5mm vertical perforation diameter with 5 horizontal perforations having 4mm diameter on each pin, Fig. 2(d). In all cases, the pin fin array contains 14 pins of 8mm diameter and 50mm height spaced uniformly at 25mm in lengthwise and spanwise pitch. The pin array is placed directly at the bottom of the vertical inlet channel.

The symmetry in the computational domain allows half of the channel to be analysed and unstructured grids are used. The channel and pins are assumed to be made of aluminum with thermal conductivity of $202 Wm^{-1}K^{-1}$. All the walls except the heating surface are treated as adiabatic. Four different inlet velocities are selected: 5, 10, 15 and $20 ms^{-1}$, with an inlet air temperature of 300K. The outlet pressure is considered atmospheric. No-slip boundary is applied to the walls as well as all the pin fin arrays. A constant heat flux of $6000 Wm^{-2}$ supplies energy under the heat sink, Fig. 1. Laminar model is selected to particularly focus at the thermal dissipative performance of the pin fin arrays. Physical properties are assumed constant.

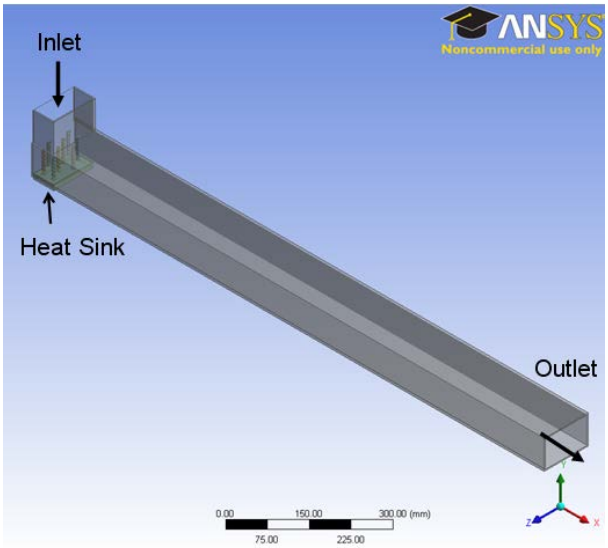

Fig. 1: 3D Numerical Model

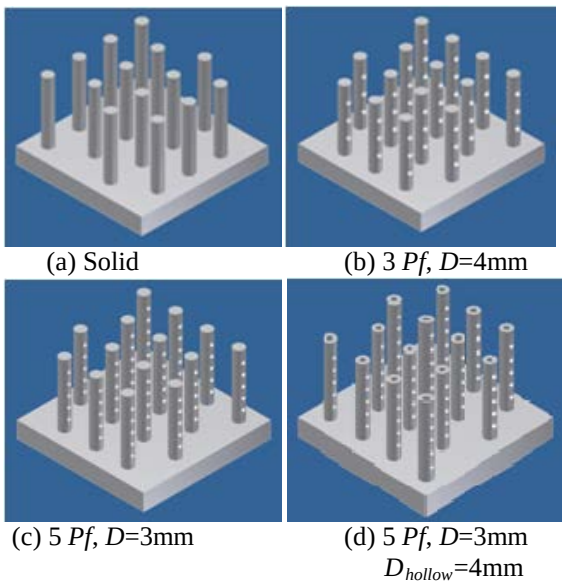

(a) Solid (b) 3 *Pf*, *D*=4mm

(c) 5 *Pf*, *D*=3mm (d) 5 *Pf*, *D*=3mm D_{hollow}=4mm

Fig. 2: Pins with Different Perforation Number (*Pf*), Horizontal Diameters (*D*) and Vertical Diameters (D_{hollow})

The following are the governing equations,

Steady-state Navier-Stokes equations,

$$\rho\left(u\frac{\partial u}{\partial x}+v\frac{\partial u}{\partial y}+w\frac{\partial u}{\partial z}\right)=-\frac{\partial P}{\partial x}+\mu\left(\frac{\partial^2 u}{\partial x^2}+\frac{\partial^2 u}{\partial y^2}+\frac{\partial^2 u}{\partial z^2}\right) \quad (1)$$

$$\rho\left(u\frac{\partial v}{\partial x}+v\frac{\partial v}{\partial y}+w\frac{\partial v}{\partial z}\right)=-\frac{\partial P}{\partial y}+\mu\left(\frac{\partial^2 v}{\partial x^2}+\frac{\partial^2 v}{\partial y^2}+\frac{\partial^2 v}{\partial z^2}\right) \quad (2)$$

$$\rho\left(u\frac{\partial w}{\partial x}+v\frac{\partial w}{\partial y}+w\frac{\partial w}{\partial z}\right)=-\frac{\partial P}{\partial z}+\mu\left(\frac{\partial^2 w}{\partial x^2}+\frac{\partial^2 w}{\partial y^2}+\frac{\partial^2 w}{\partial z^2}\right) \quad (3)$$

Heat conduction equation for the channel walls and pins,

$$\frac{\partial^2 T}{\partial x^2}+\frac{\partial^2 T}{\partial y^2}+\frac{\partial^2 T}{\partial z^2}=0 \quad (4)$$

Conservation of Energy equations for the working fluid,

$$\rho\cdot c_p\left(u\frac{\partial T}{\partial x}+v\frac{\partial T}{\partial y}+w\frac{\partial T}{\partial z}\right)=\lambda\left(\frac{\partial^2 T}{\partial x^2}+\frac{\partial^2 T}{\partial y^2}+\frac{\partial^2 T}{\partial z^2}\right) \quad (5)$$

The Continuity equation,

$$\frac{\partial u}{\partial x}+\frac{\partial v}{\partial y}+\frac{\partial w}{\partial z}=0 \quad (6)$$

where ρ is the air density, P the pressure, μ the viscosity, T the temperature, c_p the specific heat capacity of air, λ the thermal conductivity, (u, v, w) the velocity components, and (x, y, z) the coordinates.

SIMPLE algorithm is used to couple pressure and velocities. The fluid flow and heat transfer are determined by solving iteratively the governing energy and momentum equations in Eq.1-6. The convergence criteria are set to 10^{-3} for mass conservation together with three velocity components, and at 10^{-6} for energy equation. Simulations have been carried out with triangular meshes within 1.3×10^6 to 3.5×10^6 elements to ensure grid independent solutions. The highest number of element is used for all the simulations. The calculated results confirm that the variations of the surface temperature distributions along the heat sink surface are smaller than 2^oC. Validations of the numerical simulations are given in a companion study [11].

The average Nusselt number, $\overline{Nu}$, overall thermal efficiency, η, pressure drop, ΔP, friction factor, f, and Reynolds Number, Re_p, are defined as follow,

$$\overline{Nu} = \frac{q'' D_h}{k_{air}\left(\overline{T_w} - \frac{T_{out} + T_{in}}{2}\right)} \tag{7}$$

$$\Delta P = P_{in} - P_{out} \tag{8}$$

$$\eta = \frac{\overline{Nu}}{\Delta P} \tag{9}$$

$$f = \frac{\Delta P}{\left(\frac{L}{D_h}\right)\left(\frac{1}{2}\rho \cdot u_o^2\right)} \tag{10}$$

$$Re_p = \frac{\rho u_o D_p}{\mu} \tag{11}$$

where $\overline{T_w}$ is the average base plate temperature, T_{in} the inlet temperature, T_{out} the outlet temperature, k_{air} the thermal conductivity of air, q'' the heat flux, D_h the hydraulic diameter of the inlet rectangular channel, D_p the pin fin diameter, u_o the inlet velocity, L the impinging affected distance between the inlet pressure P_{in} and outlet pressure P_{out}. The related thermophysical properties of air are obtained using the bulk mean temperature,

$$T_m = \frac{T_{in} + T_{out}}{2} \tag{12}$$

3.0 Results and Discussion

3.1 Pressure Drop Effect

Fig. 3 shows the effects of the number of perforation, horizontal perforation diameter (D), and vertical perforation diameter (D_{hollow}) on f, as a function of Re_p. In Fig. 3a, friction factor decreases with increasing Re_p due to the increase in kinetic energy of the flow (see Eq.10). Since pin fin arrays restrict the fluid flow passage causing much energy dissipation, f are higher for both solid and perforated pin fin arrays when compared with that in the smooth channel. Figs. 3(a), (b) and (c) also shows that f decreases with increasing number of perforation as the perforations decrease the blockage effect.

Since the number of perforation is restricted on a given pin, f may be further reduced by increasing the perforation diameter. It is important to note that vertically perforated pins are critical for heat sinks subject to impinging flow. As shown in Fig. 3(d) pins with horizontal and vertical perforations have lower f than pins without, and pins with vertical perforations have the lowest f. Thus, at $Re_p = 8\times10^3$, pin fin arrays with 5Pf, D=3mm, and D_{hollow} from 2, 3, 4 to 5mm diameter recorded f which are 7%, 8%, 9% and 10%, respectively, lower than that using solid pin fin array. Solid pin fin array presents a higher impedance than perforated pins; the resulting wake would also be larger causing higher

pressure losses. As a result, it is evident that smaller f can be effectively achieved using perforated pin fins.

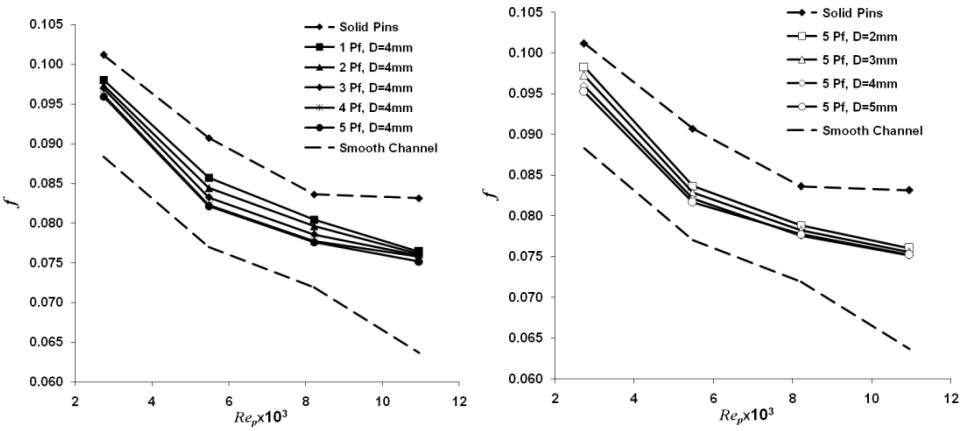

(a) Number of Perforation (Pf)

(b) Horizontal Perforation Diameter (D)

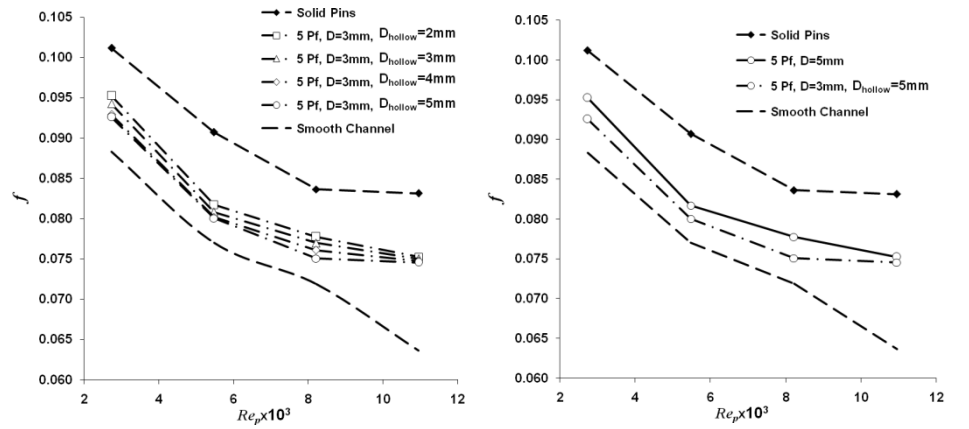

(c) Vertical Perforation Diameter (D_{hollow})

(d) Pins With and Without Vertical Perforations

Fig. 3: The Effect of Number of Perforation, Horizontal, and Vertical Diameters on Pressure Drop

3.2 Heat Transfer Performance

The effects of the number of perforation, horizontal diameter, and horizontal and vertical perforation diameter on $\overline{Nu}/\overline{Nu_s}$ are shown in Figs. 4(a), (b), and (c), respectively; where $\overline{Nu_s}$ is the Nusselt number of smooth channel. Fig. 4(a) clearly suggests that $\overline{Nu}/\overline{Nu_s}$ increases with increasing Re_p . The solid and perforated pin fins heat sinks provide much higher thermal dissipation compared with the smooth channel without pin fin. More importantly, thermal dissipation is higher with perforated pin fins than with solid pins. It is found that the larger the number of perforation on each pin fin the higher the $\overline{Nu}$. Such effect is due to the increase in heat transfer surface area when the number of perforation

increases. Fig. 4(b) shows the effect of horizontal perforation diameter on pin fins with five perforations. The simulations show that increasing the perforation diameter from 2 to 3mm increases $\overline{Nu}$. However, further increasing the perforation diameter from 4 to 5mm reduces $\overline{Nu}$. Fig. 4(c) shows the effect of horizontally and vertically perforated pins with 5 horizontal perforations of 3mm diameter. It is clear that increasing the vertical perforation diameter from 2mm to 3mm increases $\overline{Nu}$, but further increasing it to 4mm reduces $\overline{Nu}$. Thus, when the perforation diameter is greater than 3mm, either horizontally or vertically $\overline{Nu}$ decreases. This is due to the decrease in the cross sectional area of the pin for heat conduction along the pins. As shown in Fig. 4(d), by coupling the effect of horizontal and vertical perforations, the heat transfer performance of the pins may be optimized. Maximum heat transfer is obtained for pin fins with 5*Pf*, *D*=3mm, and D_{hollow}=3mm, e.g., at $Re_p = 11\times10^3$ the $\overline{Nu}$ is 9.2% higher than that with solid pins.

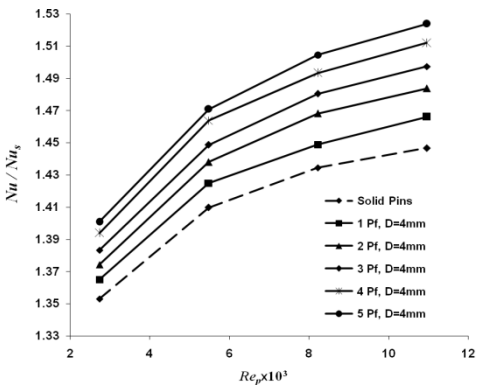

(a) Number of Perforation (*Pf*)

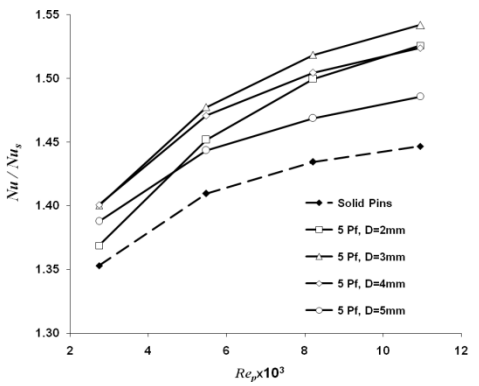

(b) Horizontal Perforation Diameter (*D*)

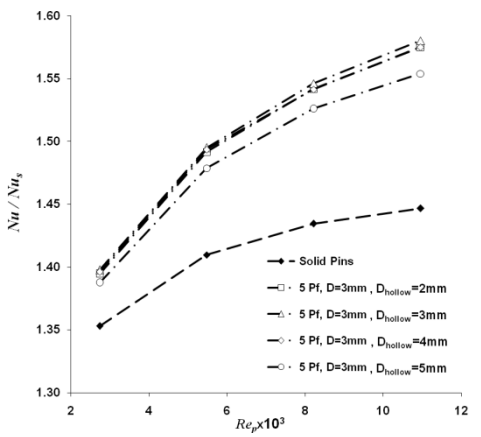

(c) Vertical Perforation Diameter (D_{hollow})

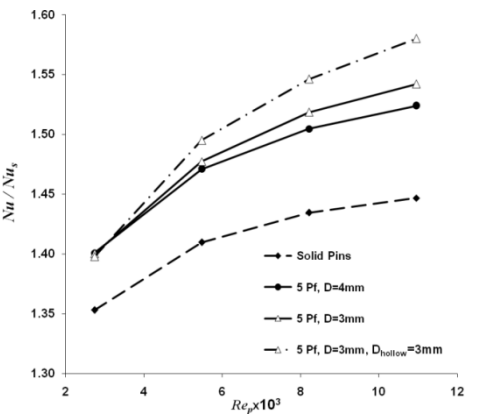

(d) Pins With and Without Vertical Perforations

Fig. 4: $\overline{Nu}$ vs. Re_p : The Effect of Number of Perforation, Horizontal, and Vertical Diameters

3.3 Heat Transfer Efficiency

Overall thermal efficiency is defined by the ratio of $\overline{Nu}$, over ΔP [12] with unit Pa^{-1}. It describes the relative cost (pressure drop hence pumping power) to achieve a certain rate of heat transfer. Fig. 5 shows the range of the overall thermal efficiency for two perforated pin fin arrays which are the best performing in each case. It is found that the perforated pin fins have higher efficiency than the solid pin fins. Clearly pin fin arrays that couple both horizontal and vertical perforations are able to further enhance the thermal dissipative performance when subject to vertical impinging flow whilst lowering the pumping power needed by the heat sink. Since pressure drop significantly affects the thermal efficiency of a heat sink, perforated pin fin array on the heat sink may maximize the rate of heat transfer at minimal cost.

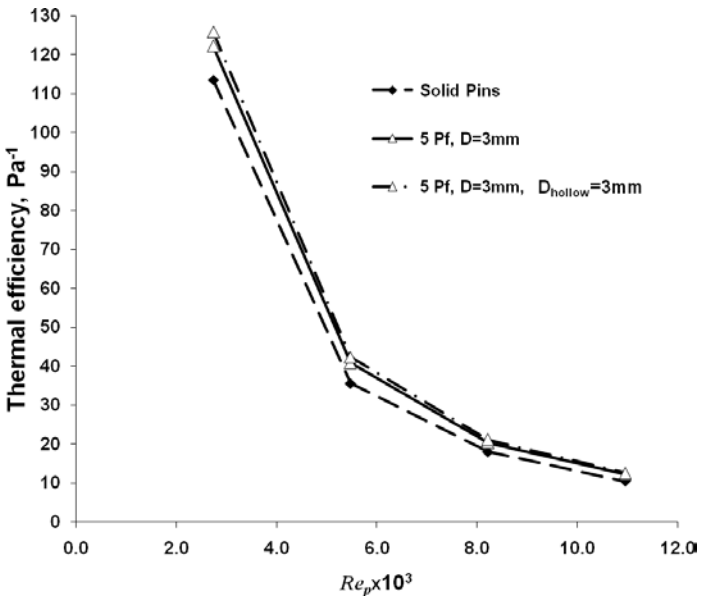

Fig. 5: Dependent of Thermal Efficiency on the Number of Perforation, Horizontal Diameter, and Vertical Diameter

3.4 Comparison: Effects of Number of Perforation and Perforation Diameter

The geometry and dimensions of the pin fin limit the number of perforations and perforation diameter that may be used. Thus, it is important to look into the relative contribution of both effects on heat transfer on pin fin array with the same surface area. In Fig. 6(a) the pin fin array with three perforations of 4mm diameter is compared with five perforation of 2mm diameter. It is found that at $Re_p > 5.5\times10^3$ the latter produced a higher $\overline{Nu}$ hence a higher thermal dissipation rate. The difference may be explained by the present flow impinging effect as it is more difficult for the flow stream to bend horizontally into a smaller perforation at a lower Re_p, especially for 5 *Pf* pins where the first and second perforations are too close to the heated surface. However, further increasing the surface area as well as perforation diameter, as shown in Fig. 6(b), the rate of heat transfer is higher for pins with five perforation of 3mm diameter than that with three perforation of

4mm diameter. Thus, effective pin area for axial heat conduction along the pin is larger for pins with smaller perforations, provided that Re_p>5.5×10^3 when the first perforation of D=2mm is 9mm above the heat sink surface.

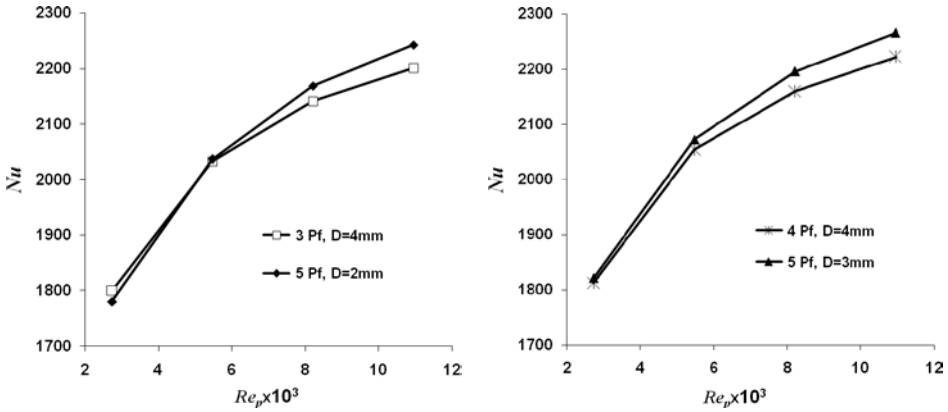

(a) 3 *Pf*, *D*=4mm vs. 5 *Pf*, *D*=2mm (b) 4 *Pf*, *D*=4mm vs. 5 *Pf*, *D*=3mm

Fig. 6: Effect of Number of Perforation and Horizontal Perforation Diameter at An Equivalent Pin Fin Array Surface Area of 0.031m^2 (a) and 0.032m^2 (b) Respectively

Larger number of perforations may reduce the blockage effect on the flow producing smaller but also larger number of wakes behind the pins [11, 12]. This may be seen in Figs. A1 and A2. These smaller wakes are more effective in removing the fluid away from the pins and carrying the heat with it. Fig. A3 also show that temperature is generally lower in perforated pins (5 *Pf*, *D*=3mm, D_{hollow}=3mm) than that in the solid pins. As a result, the number of perforation is more critical in enhancing thermal dissipation than the perforation diameter.

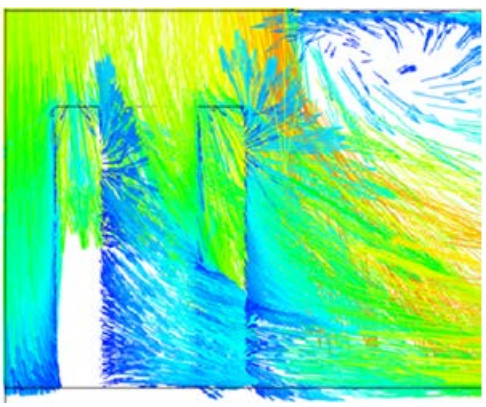

Fig. A1: Wakes Behind Solid Pin Fins

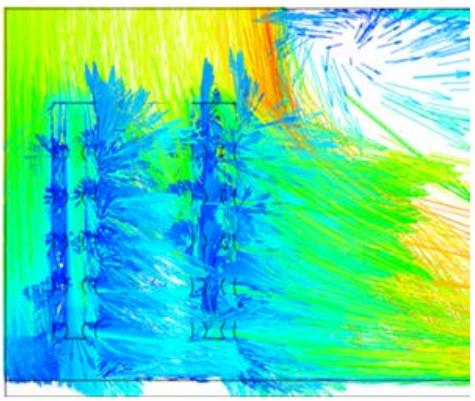

Fig. A2: Wakes Behind Perforated Pin Fins

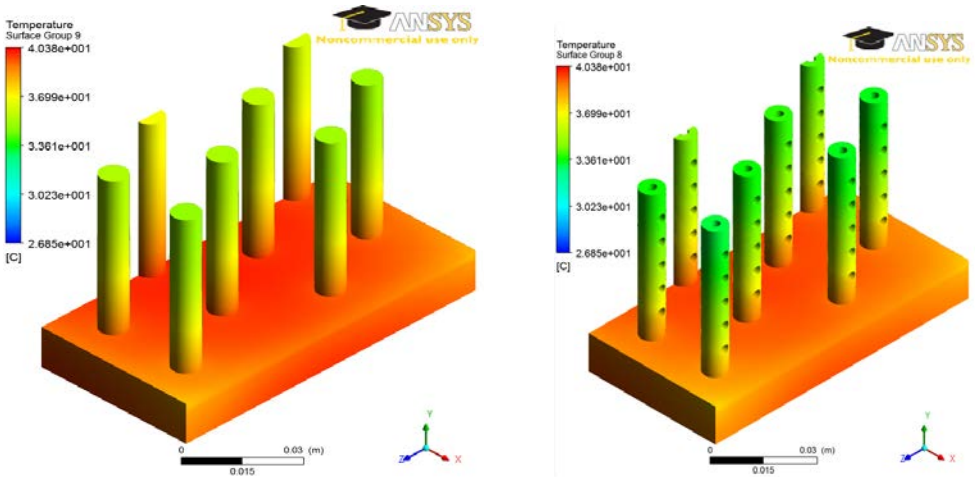

(a) (b)

Fig. A3: Three Dimensional Temperature Distributions between (a) Solid Pins and (b) Pins with Horizontal and Vertical Perforations

4.0 Conclusion

Steady-state forced convective heat transfer in staggered pin fin arrays in a rectangular channel has been studied using numerical simulation to quantify their heat transfer characteristics. Thermal efficiencies are compared between solid and various perforated pin fin heat sinks. The conclusions of this study are:

1. ΔP across the heat sink is smaller with increasing number of perforation and perforation diameter. In all cases, perforated pin fin array performs better than the solid pins. Hence, perforated pin fins require less pumping power than the solid pins for the same thermal performance.

2. Maximum $\overline{Nu}$ is obtained from pin fin array with 5 perforations, 3mm horizontal perforation diameter, and 3mm of vertical perforation. It is approximately 9% higher than that for the solid pins at Re_p=11×10^3. More importantly, the thermal energy is dissipated at a smaller pressure drop.

3. $\overline{Nu}$ increases with the increasing (i) number of perforation, (ii) horizontal perforation diameter, and (iii) coupling horizontal and vertical perforation diameters. Further increasing the perforation diameters will lead to a reduction in thermal dissipation. This is due to the decrease in vertical heat conduction along the perforated pin fins, as well as the perforations induces reshaping of wakes behind the pins. Thus, while designing a perforated pin fin array, the balance between the perforation number and diameter should be carefully taken into consideration.

5.0 Acknowledgement

The authors would like to thank SEGi University College (Kota Damansara) for the financial support of the research project (SCM-005644).

REFERENCES

1 D.K. Kim, S.J. Kim and J.J. Bae. *International Journal of Heat and Mass Transfer*. **52**, 3510-3517 (2009).

2 Z.Q. Lou, A.S. Mujumdar and C. Yap. *Applied Thermal Engineering*. **25**, 2687-2697 (2005).

3 Y.T. Yang and H.S. Peng. *International Journal of Heat and Mass Trasnfer*. **52**, 3473-3480 (2009).

4 E.M. Sparrow, J.W. Ramsey and C.A.C. Altermani. *ASME Journal of Heat Transfer*. **102**, 44-50 (1980).

5 M. Tahat, Z.H. Kodah, B.A. Jarrah and S.D. Probert. *Applied Energy*. **67**, 419-442 (2000).

6 D. Soodphakdee, M. Behnia and D.W. Copeland. *The International Journal of Microcircuits and Electronic Packaging*. **24**, 68-76 (2001).

7 J. Yang, M. Zeng, Q. Wang and A, Nakayama. *ASME Journal of Heat Transfer*. **132**, 051702-1–051702-8 (2010).

8 B. Sahin and A. Demir. Energy *Conversion and Management*. **49**, 1684-1695 (2008).

9 Y. Rao, C. Wan, Y. Xu and S.S. Zang. *International Journal of Thermal Sciences*. **50**, 2277-2289 (2011).

10 K.K.T. Yong, Y.L. Lai, J.J. Foo and S.B. Chin. 2nd International Conference on Mechanical and Manufacturing Engineering, Malaysia (2011).

11 S.Y. Pui, Final Year Research Thesis, SEGi University College (2011).

12 H.R. Seyf and M. Layeghi. *ASME Journal of Heat Transfer*. **132**, 071401-1–071401-9 (2010).

Nomenclature

c_p	specific heat capacity, $Jkg^{-1}K^{-1}$
D	horizontal perforation diameter, mm
D_{hollow}	vertical perforation diameter, mm
D_p	pin fin diameter, mm
D_h	hydraulic diameter, mm
f	friction factor
k_{air}	thermal conductivity of air, $Wm^{-1}K^{-1}$
L	impinging affect distance, m
$\overline{Nu}$	Nusselt number
q''	heat flux, Wm^{-2}
T_{in}	inlet temperature, ^oC
T_m	bulk mean temperature, ^oC
T_{out}	outlet temperature, ^oC
$\overline{T_w}$	average base plate temperature, ^oC
P	air pressure, Pa
ΔP	pressure drop, Pa
Pf	number of perforation
P_{in}	pressure inlet, Pa
P_{out}	pressure outlet, Pa
Re_p	Reynolds number based on pin fin diameter
u_o	inlet velocity, ms^{-1}
u, v, w	velocity components, ms^{-1}
x, y, z	coordinates

Greek symbols

η	thermal efficiency, Pa^{-1}
ρ	density of air, kgm^{-3}
μ	viscosity of air, $kgm^{-1}s^{-1}$